

Dynamics of phospholipid tubules in a concentrated solution: Results from high-field magnetic birefringence and quasielastic light scattering

S. Sprunt, G. Nounesis, and J. D. Litster

Francis Bitter National Magnet Laboratory, Massachusetts Institute of Technology, Cambridge, Massachusetts 02139-4307

B. Ratna* and R. Shashidhar

Biomolecular Science and Engineering, Code 6090, Naval Research Laboratory, Washington, D.C. 20375

(Received 4 November 1992)

The dynamical diffusion of phospholipid tubules in highly concentrated solution has been studied as a function of temperature by high-field magnetic birefringence and by dynamic light scattering in zero field. Data at a temperature well below the lipid chain-melting transition $T = T_m$ are analyzed using theoretical predictions for rigid-rod dynamics. While qualitatively successful, these lead to an estimate of the rotational diffusion constant which is larger than that anticipated when dynamical rod entanglement in a homogeneous solution is the only effect considered at high concentration. For $T \rightarrow T_m$, the results from both experimental techniques exhibit a marked temperature dependence, revealing dynamical studies to be a sensitive and potentially interesting probe of the phase transformation at T_m .

PACS number(s): 61.30.Eb, 61.30.Gd, 87.15.Da

When a phospholipid solution with some aqueous content is cooled below the lipid chain-melting temperature T_m , a remarkable, hollow cylindrical structure called a tubule may spontaneously form [1]. Lipid tubules are rigid, highly anisotropic particles with quite large dimensions for self-assembled structures; they are typically a few tens to several hundred microns in length L and a few tenths to one micron in diameter b , and have wall thicknesses of one to several bilayers. In a weakly aqueous solution, these dimensions may be controlled with minimal polydispersity [2]. Theoretical models [3] for tubule stability at $T < T_m$ focus on the establishment within the bilayer of orientational or positional order characterized by an anisotropic elasticity; hence the lipid chains are expected to be tilted with respect to the bilayer normal. In fact, x-ray diffraction studies [4] confirm this in specific systems. More generally, morphological studies suggest that either large vesicles (liposomes) [5] or loosely wound, helical bilayer structures [6] may be tubule precursors; in the latter case, the tubules develop fully only at $T \ll T_m$, and the helicity arises from molecular chirality.

However, the detailed physics of tubule formation, together with quantitative measurements of the process, is largely an outstanding issue. In another paper [7], we present a quantitative investigation of the phase transformation of highly concentrated tubules at T_m using high-field magnetic birefringence and samples composed of the phospholipid 1,2-bis(10,12-tricosadiynoyl)-sn-glycero-3-phosphocholine (abbreviated DC_{8,9}PC) in an 85%:15% (by weight) methanol:water solution. For this system, the tubules have $L \approx 60 \mu\text{m}$, $b \approx 0.4 \mu\text{m}$, and single-bilayer wall thickness [2]. From analysis of microscopy data, these dimensions are found to be highly uniform. The diameter and wall thickness are essentially constant, and variance of L is less than $6 \mu\text{m}$ [8]. For $T \rightarrow T_m$, we ob-

serve substantial pretransitional behavior in the induced refractive-index anisotropy Δn at high field. In the present paper, we demonstrate that the dynamical properties of solutions with tubule concentration ν near ν^* , studied by high-field magnetic birefringence (MB) and zero-field dynamic light scattering (DLS), also reveal quite marked pretransitional effects when $T \rightarrow T_m$. Here ν^* is the concentration at which an isotropic system of hard rods is expected to become nematic [9]. More generally, our results indicate that lipid tubules are an important system for the study of hard-rod dynamics, which is unique in that the particles are of very large size (and hence have long diffusion times), that they have sufficient magnetic-susceptibility anisotropy to be completely aligned in currently available fields, and that they do not aggregate significantly [4,6] even at quite high concentration. Our work represents a preliminary study, which suggests an interesting direction for more extensive experimentation and the need for more detailed modeling of the tubule-transformation process.

The equilibrium dynamical behavior of hard rods in solution has been the subject of substantial theoretical [9] and experimental [10–14] investigation since the classic paper of Onsager [15] on the statistical mechanics of such systems. The dynamics of rigid cylinders with $L \gg b$ may be classified by the particle concentration ν [9]. For $\nu \leq L^{-3}$, the “dilute” limit, the dynamics are those of a single particle in a Brownian potential. When $L^{-3} < \nu < (bL^2)^{-1}$, the “semidilute” case, the form of the single-particle diffusion equation remains valid so long as the system is locally isotropic; however, the diffusion constant is expected to be considerably modified by the topological constraint that the particles cannot cross through one another. In the “concentrated” regime $\nu \sim (bL^2)^{-1}$, where the solution may contain mixture of nematic and isotropic domains, steric interactions and local anisotro-

py must be considered explicitly in the diffusion equation, which, as a result, becomes quite complicated.

The methanol-water-tubule samples studied in the present work were prepared at the Naval Research Laboratory; the tubules were precipitated [2,4] from a DC_{8,9}PC dispersion in pure methanol upon addition of water and lowering of the temperature below $T_m \approx 33.2^\circ\text{C}$ [16]. The original lipid mass densities were $\rho = 2.0 \text{ mg/cm}^3$ (MB experiment) and $\rho = 1.0 \text{ mg/cm}^3$ (DLS experiment), corresponding approximately [17] to $v \sim (1.5-3.0) \times 10^9 \text{ cm}^{-3}$, very near the upper limit for a concentrated isotropic phase [7]. Care was taken to minimize the exposure of the samples to room light and to avoid cross-linking of the diacetylene groups. Cross-linking results in an orange coloration of the sample and an upward shift in T_m . Neither effect was observed in the samples studied here. Our experiments were performed promptly on well-mixed samples, over relatively short periods ($< 3 \text{ h}$), and with frequent changes in temperature and magnetic field. The formation of tubule "logjams" was observed to be significant only over relatively long times ($\sim 24 \text{ h}$) and only if the sample was kept still at constant T and $H = 0$. Details of the apparatus for very high-field, high-sensitivity MB measurements have been given elsewhere [7]. The DLS apparatus is a standard one for homodyne correlation spectroscopy.

Because the phosphate group of the lipid may become protonated in a partially aqueous solution, the possibility of Coulombic interparticle interactions, in addition to steric (hard-rod) repulsions, must be considered. However, it has recently been established [18] that at neutral pH and even in purely aqueous solution, the net lipid charge due to association of H^+ ions is sufficiently small so that the Coulomb barrier is less than or comparable to the thermal energy $k_B T$, and the effective range of the Coulomb force is short compared to both the large tubule diameter ($0.4 \mu\text{m}$) and the typical interparticle spacing ($\sim 15 \mu\text{m}$). In this case, the dynamical behavior is dominated by topological constraints, and the effect of a weak Coulomb repulsion may be incorporated by assuming a slightly larger effective tubule diameter in the usual hard-rod potential.

The quantities we have studied are the optical refractive-index anisotropy $\Delta n(t) = \Delta n_{\text{max}} S(t)$, where S is the orientational order parameter (experimentally induced by an external magnetic field \mathbf{H}), and the intensity-intensity autocorrelation function for polarized scattered light $G_{VV}(\mathbf{q}, t) = \langle I_{VV}(\mathbf{q}, 0) I_{VV}(-\mathbf{q}, t) \rangle$ at wave-vector transfer \mathbf{q} . The depolarized scattering G_{VH} , which couples mainly to rotational diffusion, is down by several orders of magnitude [11] for rods with a small polarizability anisotropy $\Delta\alpha$, $G_{VH}/G_{VV} \sim (\Delta\alpha)^2 / (\alpha_{\parallel} + 2\alpha_{\perp})^2 \ll 1$. For large particles like tubules, G_{VH} would also be expected to have a relaxation time that is too long to be studied by correlation spectroscopy.

$\Delta n(t)$ [9] and $G_{VV}(\mathbf{q}, t)$ [19] are given by

$$\Delta n(t) = \Delta n_{\text{max}} \int \int_V d\mathbf{R} d\mathbf{u} (u_z^2 - u_x^2) \Psi(\mathbf{R}, \mathbf{u}; t), \quad (1)$$

$$G_{VV}(\mathbf{q}, t) = A [\langle v_{-\mathbf{q}}(0) v_{\mathbf{q}}(t) \rangle^2 - \langle |v_{\mathbf{q}}(0)|^2 \rangle^2], \quad (2)$$

with

$$\begin{aligned} \langle v_{-\mathbf{q}}(0) v_{\mathbf{q}}(t) \rangle &= \int \int_V \int \int_V d\mathbf{R} d\mathbf{u} d\mathbf{R}' d\mathbf{u}' \exp[i\mathbf{q} \cdot (\mathbf{R} - \mathbf{R}')] \\ &\quad \times \frac{\sin(\mathbf{Q} \cdot \mathbf{u})}{(\mathbf{Q} \cdot \mathbf{u})} \frac{\sin(\mathbf{Q} \cdot \mathbf{u}')}{(\mathbf{Q} \cdot \mathbf{u}')} \\ &\quad \times \langle \Psi(\mathbf{R}, \mathbf{u}; 0) \Psi(\mathbf{R}', \mathbf{u}'; t) \rangle \end{aligned} \quad (3)$$

for tubule density fluctuations $v_{\mathbf{q}}$ and $\mathbf{Q} = \mathbf{q}L/2$. In these equations, \mathbf{u} is a unit vector along the tubule long axis (\mathbf{z} is taken as the direction of an external aligning field \mathbf{H}), \mathbf{R} is the tubule center-of-mass coordinate, V is the illuminated volume, A is an empirical constant that depends on the average tubule density, the tubule polarizability, and details of the DLS apparatus, and $\Psi(\mathbf{R}, \mathbf{u}; t)$ is the time-dependent combined positional and orientational particle distribution function. The sinusoidal factors in (3) account for the phase differences in the light scattered from different points along the tubule length; additional phase factors due to the finite tubule wall thickness $\delta \approx 5 \times 10^{-7} \text{ cm}$ may be set to unity since $q\delta \ll 1$.

The spatial and temporal evolution of Ψ for concentrations up to the liquid-crystalline phase may be described by a Smoluchowski equation given by Doi *et al.* [9,20],

$$\begin{aligned} \frac{\partial \Psi}{\partial t} &= \nabla [D_{\parallel} \mathbf{u} \mathbf{u} + D_{\perp} (\mathbf{I} - \mathbf{u} \mathbf{u})] [\nabla \Psi + \Psi \nabla (U_{\text{MF}} + U_{\text{ext}})] \\ &\quad + \mathcal{R} D_r (\mathbf{u}) [\mathcal{R} \Psi + \Psi \mathcal{R} (U_{\text{MF}} + U_{\text{ext}})], \end{aligned} \quad (4)$$

where the operators $\nabla = \partial/\partial \mathbf{R}$ and $\mathcal{R} = \mathbf{u} \times \partial/\partial \mathbf{u}$. In this expression, the interparticle interaction is expressed by a mean-field, excluded-volume potential [9]

$$U_{\text{MF}}(\mathbf{R}, \mathbf{u}; t) = 2vbL^2 \int \int_V d\mathbf{R}' d\mathbf{u}' |\mathbf{u} \times \mathbf{u}'| \Psi(\mathbf{R}', \mathbf{u}'; t),$$

which accounts for the steric repulsions between rods. The single-particle interaction with an external magnetic field is

$$U_{\text{ext}}(\mathbf{u}; t) = -\frac{1}{2} \Delta\chi H^2 u_z^2.$$

The first term in (4) accounts for translational diffusion of the tubules; the associated diffusion constants are D_{\parallel} for motion along the tubule axis \mathbf{u} and D_{\perp} for motion perpendicular to \mathbf{u} . The second term accounts for rotational diffusion with diffusion constant D_r . In very concentrated solutions, where local orientational anisotropy may be expected, the constraint of no tubule interpenetration implies a dependence of D_{\perp}, D_r on \mathbf{u} [9,21]. (Because of the large tubule aspect ratio, D_{\parallel} is unaffected.) The dynamical equation thus contains a nonlinear dependence on Ψ , making the general calculation of (1) and (2) a very difficult problem.

Analytic results may, however, be obtained for certain limiting cases. We will concentrate on those of interest for our analysis below. For $v \sim v^*$, Eq. (4) incorporates the following: (1) mean-field interactions; (2) the possibility for inhomogeneity in the spatial distribution (Ψ depends on \mathbf{R}); and (3) dynamics dependent on tubule orientation \mathbf{u} because of local entanglement effects. The prob-

lem of rotational diffusion has been solved rigorously [21] for a concentrated, homogeneous hard-rod system in the isotropic phase by dropping the conditions (1) and (2), and treating (3). The results, obtained for relaxation of the orientational order parameter after removal of a large applied field H , where $\Delta\chi H^2 \gg k_B T$, are [21]

$$S(t) \approx \exp\left[-\frac{3}{2}(2\alpha_1 D_r)^{1/2} t^{1/2}\right], \quad (5a)$$

$$S(t) \approx \exp(-6D_r t) \quad (5b)$$

for $S \approx 1$ ($t \rightarrow 0$) and $S \approx 0$ ($t \rightarrow \infty$), respectively. Also, α_1 is a constant, $\alpha_1 \approx 0.33$ [21], and [19]

$$D_r = \frac{D_{r0}}{1 + \beta_r (\nu L^3)^2}, \quad (6)$$

where β_r is an empirical parameter, $\beta_r \ll 1$, and D_{r0} is the rotational diffusion constant for a dilute solution [22],

$$D_{r0} = \frac{3k_B T [\ln(L/b) - 0.8]}{\pi \eta_S L^3}, \quad (7)$$

with solvent viscosity η_S . For our tubules in methanol-water at 25°C, we get $D_{r0} \approx 7.7 \times 10^{-5} \text{ sec}^{-1}$. Equations (5) show that the functional form of $S(t)$ depends on its magnitude, a result of condition (3) above. Equation (6) expresses a second effect, that of rod entanglement, on the diffusion constant, which may be important even for $\nu \ll \nu^*$ [9]. For hard-rod systems, β_r is typically found [10,23] to be rather small, $\beta_r \sim 10^{-4} - 10^{-3}$, and has been reported [11,24] as low as 5×10^{-5} . Thus, in real systems, entanglement effects are in fact suppressed until quite high semidilute concentrations are reached.

For $\nu \rightarrow \nu^*$, the mean-field interaction U_{MF} becomes important. In a homogeneous solution, where Ψ is a function of \mathbf{u} only, dynamical mean-field arguments predict [9] that $D_r \rightarrow D_r^*(1 - \nu/\nu^*)$ in Eq. (5b) for the decay of $S(t)$ upon removal of a *weak* applied field. Thus, the orientational response time $\tau \propto D_r^{-1}$, measured for small H , should increase significantly on approach to ν^* ; this has been demonstrated [25] in a hard-rod system with L and b about 100 times smaller than for tubules. A true divergence, however, is not experimentally observable because of phase separation into nematic and isotropic domains when $\nu \rightarrow \nu^*$. Such separation would lead to sample inhomogeneity, and consequently to a dependence of Ψ on the positional coordinate \mathbf{R} . If this dependence is substantial, an analysis based on a strict decoupling of rotational and translational motion would not be applicable, and the mean-field effects on D_r may differ from the case of an ideal homogeneous solution. The problem of coupled rotational-translational diffusion, given by Eq. (4), has been treated [19] in the calculation of the DLS correlation function G_{VV} [Eq. (2)] for a concentrated isotropic system ($\nu < \nu^*$, $S \sim 0$). When $q \sim 0$, the results are similar to those obtained for a semidilute system, except that the diffusion constants are *enhanced* by a factor $1 + 8\nu/\nu^*$. DLS experiments on a rigid-rod polymer system at large ν have in fact confirmed this enhancement [14]. Thus, when $\nu \rightarrow \nu^*$, and if the phase-coexistence region is particularly large (suppressing the pretransitional

effects), the tendency for D_r to decrease due to orientational order may be offset by the effects of sample inhomogeneity in general and coupling to translational diffusion in particular.

We now consider specific predictions for DLS that are relevant for tubules. Detailed treatments of the problem for hard rods have been given [11,19,26] with the neglect of only condition (3) above, an approximation that may not be too severe for $\nu < \nu^*$ and $U_{\text{ext}} \sim 0$. The key parameter [9,26] in the analysis is the ratio $\gamma = (D_{\parallel} - D_{\perp})q^2/D_r \approx \beta_r^{-1}(qL)^2$. For $\gamma \leq 10$, the correlation function $G_{VV}(t)$ may be accurately modeled as a discrete sum of exponentials [11,13]. For $\gamma > 10$, however, $G_{VV}(t)$ is characterized by a continuous distribution of decay constants [9,21]; if the limit $qL \gg 1$ also applies, a three-cumulant analysis

$$G_{VV}(t) = A \exp\left[-2\Gamma_1 t + \mu_2 t^2 - \frac{\mu_3}{3} t^3\right] + B \quad (8)$$

has been shown to approximate the exact behavior rather well [26]. Since tubules have $L \gg \lambda$, we indeed expect $qL \gg 1$. For our system with $L = 60 \mu\text{m}$, lab scattering angle $\theta_l = 45^\circ$, $\lambda = 6.33 \times 10^{-5} \text{ cm}$, and solution refractive index $n_s \approx 1.3$, we get $qL = (4\pi L/\lambda)n_s \sin[1/2 \sin^{-1}(\sin\theta_l/n_s)] = 44$. Moreover, since $\beta_r \ll 1$, we should have $\gamma \gg 1$. Thus, we shall use (8) to analyze the experimental DLS data for the tubules.

When $qL \gg 1$, the phase factors in (3) will oscillate very rapidly unless $q \cdot \mathbf{u}, \mathbf{u}'$ (i.e., $\mathbf{Q} \cdot \mathbf{u} \approx 0$ and $\sin(\mathbf{Q} \cdot \mathbf{u})/(\mathbf{Q} \cdot \mathbf{u}) \approx 1$, and similarly for \mathbf{u}'). DLS from a tubule solution at any reasonable θ_l will therefore probe only translational diffusion perpendicular to the rod axis. A calculation of the parameters in (8) for coupled translational and rotational diffusion at $qL \gg 1$ gives [9,26]

$$\Gamma_1(\mathbf{q}) = \left[D_{\perp}^* + \frac{L^2}{12} D_r^* \right] q^2, \quad (9a)$$

$$\mu_2(\mathbf{q}) = \frac{4}{5} \left[\frac{L^2}{12} D_r^* q^2 \right]^2, \quad (9b)$$

where the superscript * here and in the following denotes a renormalization due specifically to the mean-field interactions. Since, for a dilute solution [22], $D_{\perp} = D_{\perp 0} = k_B T \ln(L/b)/(4\pi\eta_S L)$, we have from (7), $D_{\perp 0} \approx (L^2/12)D_{r0}$. If the topological constraints in a concentrated isotropic solution have similar effects on D_{\perp} and D_r (i.e., if the form of (6) also applies to D_{\perp}), we may also have $D_{\perp} \approx (L^2/12)D_r$, and an analogous relation between D_{\perp}^* and D_r^* when $\nu \rightarrow \nu^*$. On the other hand, it has been suggested [9,21] that D_{\perp} is essentially negligible at large ν ; in that case, $D_{\perp}^* \ll (L^2/12)D_r^*$ might be expected. These two limiting possibilities for the predictions (9) will be discussed further while analyzing the experimental data below.

We now turn to our results for the relaxation of $\Delta n(t)$ after the rapid removal of a magnetic field in which the tubule alignment is saturated. Samples formed from a lipid solution with $\rho = 2.0 \text{ mg/cm}^3$ (yielding ν approximately at the theoretical upper limit for an isotropic

phase) generally showed some optical anisotropy [7] in zero field, presumably due to the presence of nematic domains. The impact of large domains on the dynamics after removal of the field from an aligned tubule state was observed to be quite dramatic, resulting in some cases in nonmonotonic behavior of $\Delta n(t)$ and more often in decays to nonzero (i.e., nonisotropic) levels of Δn .

By a combination of mixing the sample immediately prior to loading and cycling of the field between zero and levels below saturated alignment, allowing for equilibration after each change in H , a zero-field system with domain sizes much smaller than the probe beam cross section ($\sim 400 \mu\text{m}$ diameter) could be obtained. For these samples, which showed a purely overdamped response to field removal, the measured $\Delta n(t)$ should reflect the macroscopically averaged orientational dynamics of the system [as assumed in Eq. (1)]. We do observe, however, that even the best samples are not stable if left undisturbed at low temperature and zero field; some anisotropy over the illuminated volume (typically, $\sim 10\%$ of Δn_{max}) inevitably develops within a few hours. We believe that this may arise partly due to the orienting influence of the cell windows. To minimize this effect during an experimental run, we tried to avoid long periods without a field sweep or temperature change; as a result, our low-temperature data for $\Delta n(t)$ (where the decay was slowest) are limited to about one decade of decay. In any event, we considered only data that were consistent with a decay to the background level determined by heating the solution to a phase above T_m , where the structure is isotropic [7].

In Fig. 1, we present a measurement of

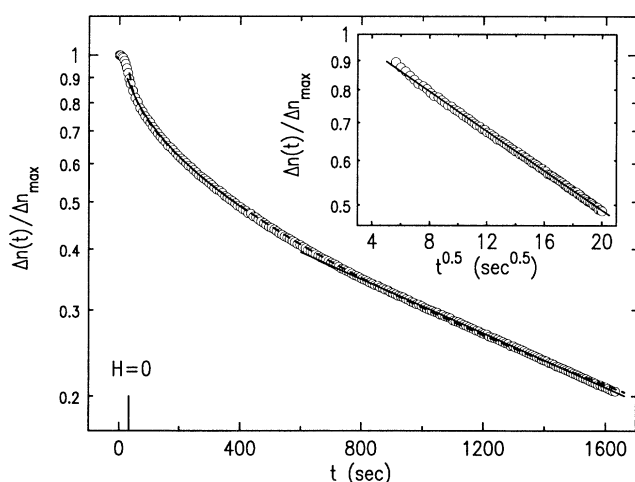


FIG. 1. Semilog plot of the decay of $\Delta n(t)/\Delta n_{\text{max}}$ for $\text{DC}_{8,9}\text{PC}$ tubules with $\rho = 2.0 \text{ mg/cm}^3$ ($\nu \sim 3 \times 10^9 \text{ cm}^{-3}$) at $T = 18.61^\circ\text{C}$. Sweepdown of a 15-T field was begun at $t = 0$; the time at which the field reached 0 T is shown. The solid lines at short and long times are the predictions of Eqs. (5) of the text. The dashed line is a fit to a stretched exponential discussed in the text. The long-time behavior is consistent with a decay to $\Delta n \approx 0$. Every other data point has been omitted for clarity. The inset shows a detail of short-time behavior for comparison with Eq. (5a).

$S(t) = \Delta n(t)/\Delta n_{\text{max}}$ from saturation ($t = 0$) after linear ramp-down of a 15-T field in 30 sec, and at a temperature $T = 18.60^\circ\text{C}$, where the tubules are fully formed, and where the initial system had $\Delta n \approx 0$ at $H = 0$. The sampling interval is 4 sec. We find $\Delta n_{\text{max}} = 3.5 \times 10^{-5}$ at 18°C . The birefringence is proportional to the polarizability anisotropy $\Delta\alpha$ of the tubules, which arises from both the shape (or “form”) and intrinsic molecular anisotropies. (Spatial fluctuations in the polarizability also account for the amplitude of scattering; indeed, the shape birefringence may be calculated from the scattering at $q = 0$ [27].) An expression for Δn_{max} for cylindrical shells with $L \gg \lambda \gg \delta$ is given in the appendix of Ref. [7]. The form birefringence is found to dominate, and reasonable agreement was obtained with the experimental Δn_{max} at low T for the tubule densities studied here; the data of Ref. [7] also show $\Delta n_{\text{max}} \propto \nu$.

The decay in the main part of Fig. 1 evidently does not follow a simple exponential over the range studied. In particular, while only recorded for $S > 0.2$, the data suggest qualitatively different behavior at shorter ($t \lesssim 400$ sec) and longer ($t \gtrsim 800$ sec) times. At long times, the data appear to fall on a single exponential, as expected from the Doi-Edwards theory [Eq. (5b)]. The solid line for $\ln S(t)$ at $t \gtrsim 750$ sec gives $D_r^* = 1.1 \times 10^{-4} \text{ sec}^{-1}$. We cannot say that this is truly the limiting value for $t \rightarrow \infty$, although in Fig. 2 we present data at higher T , which does indicate that a single exponential, extending from $S \sim 0.5$, is the limiting form. On the other hand, at short times, $t \lesssim 400$ sec, the data decay faster than a simple exponential; here the solid line in Fig. 1 represents a fit to the short-time Doi-Edwards prediction, Eq. (5a), which may be applied since $k_B T / (\Delta\chi H^2) \approx 0.003$, using

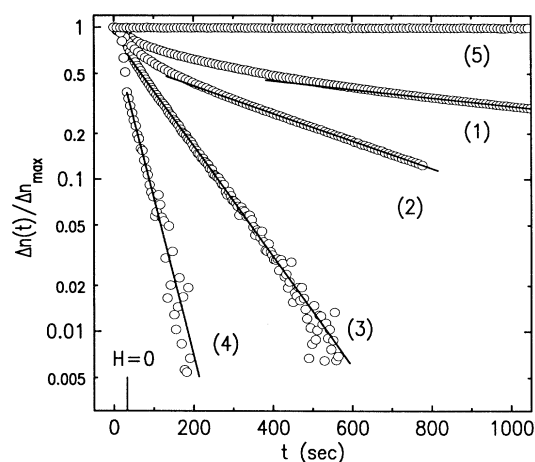


FIG. 2. Semilog plots of the decay of $\Delta n(t)/\Delta n_{\text{max}}$ as a function of temperature for $T \rightarrow T_m$ after removal of a 15-T field. The labels (1)–(4) indicate temperatures $T = 18.61, 25.95, 29.40,$ and 31.77°C , respectively. Solid lines represent single-exponential behavior at long times. Also indicated by the label (5) is the behavior of $\Delta n(t)$ for $H \rightarrow 0$ after cooling in high field from $T > T_m$ to the starting temperature $T = 18.6^\circ\text{C}$. At the lowest temperatures, every other data point has been omitted for clarity.

$\Delta\chi \approx 5.7 \times 10^{-14}$ erg/T² from Ref. [7] and $H = 15$ T. The data for $t < 30$ sec, when the field is changing, are excluded. The fit is of reasonable quality; in fact, the inset shows that the Doi-Edwards prediction, $\ln S \sim t^{1/2}$, holds rather well. However, from (5a) with $\alpha_1 = 0.33$, we find $D_r^* = 1.0 \times 10^{-3}$ sec⁻¹, about 10 times the estimate obtained from the data at larger t .

The values of D_r^* extracted by applying Eqs. (5) to the measured $\Delta n(t)$ are thus quite different. Moreover, they are anomalously large compared to the prediction based on entanglement effects alone: $D_r^* = D_r$ and, from (7), $D_r \leq D_{r0} \approx 7.7 \times 10^{-5}$ sec⁻¹ for all β_r . It is also apparent that, at least for $S \geq 0.2$, our results are not consistent with the reduction in D_r^* that would be expected on approach to ν^* in a homogeneous zero-field system. Nevertheless, the qualitatively different functional forms in Eqs. (5) are reflected in the data, and we confirm that the diffusion constant in Eq. (4) must contain an explicit dependence on the tubule orientation \mathbf{u} for large ν .

To obtain another estimate of D_r^* , we consider an alternative, phenomenological approach, which has been used to account for strong collective effects in the decay of orientational order in a highly concentrated hard-rod system [28], and which yields a single prediction for all t . In this approach, $S(t)$ is assumed to decay via a continuous distribution of dispersive modes, $W(\tau)$, where τ is the decay time for a particular mode. The distribution function W may represent a significant polydispersity—e.g., rod length (not the case for our tubules) or domain size—or account for particle interactions, whose range or nature depends on variations in local conditions—e.g., the degree of orientational anisotropy or of homogeneity in particle concentration—that arise during the decay from the aligned state. $S(t)$ is then given by

$$S(t) \approx \int_0^\infty d\tau W(\tau) \exp\left[-\frac{t}{\tau}\right], \quad (10)$$

where $W(\tau)$ is assumed to be normalized, $\int_0^\infty W(\tau) d\tau = 1$.

The choice of $W(\tau)$ is somewhat arbitrary; however, the form

$$W(\tau) = \frac{1}{\langle \tau \rangle} \exp\left[-\frac{\tau}{\langle \tau \rangle}\right] \quad (11)$$

was invoked in Ref. [28] and found to be consistent with the dynamics of a large- ν solution of cylindrical micelles. Here $\langle \tau \rangle$ is the average decay time, and also the characteristic cutoff time, of the distribution W . Combining (10) and (11), one arrives at

$$S(t) \approx \exp\left[-\left(\frac{t}{\langle \tau \rangle}\right)^{1/2}\right], \quad (12)$$

which represents a stretched-exponential time dependence. Interestingly, this expression gives a t dependence identical to that of the short-time Doi-Edwards result (7b).

More generally, one may consider in (12) an arbitrary exponent, $\alpha \neq \frac{1}{2}$. The dashed line in Fig. 1 is a two-parameter fit of the complete data for $t > 30$ sec to a

stretched exponential with α and $\langle \tau \rangle$ allowed to vary and the background fixed to zero for $t = \infty$. The results show a small but clear systematic deviation from the data at long times, $t \gtrsim 1000$ sec. We find $\alpha = 0.59$ for the exponent in (12), although the value approaches 0.5 upon range shrinking of the fit to shorter times. Thus the deviation from an exponent of 0.5 is mainly required to model the behavior at longer times. Since we did not obtain data for the final 20% of the decay, we cannot test the stretched-exponential form very rigorously for large t ; in fact, its reliability has been questioned in the asymptotic limit [28]. Assuming that all the collective effects in the tubule reorientation are accounted for simply by taking a stretched-exponential dependence, we may estimate for the dashed-line fit in Fig. 1 $D_r^* = \langle D_r \rangle \approx (6\langle \tau \rangle)^{-1} \approx 2.0 \times 10^{-4}$ sec⁻¹, which lies between the values obtained from Eqs. (5). Again we arrive at a diffusion constant for very large ν that is greater than the prediction for a concentrated isotropic phase in which there is no coupling to translational diffusion.

The large values of D_r^* obtained using both the approaches of Eqs. (5) and (10) suggest that the tubule reorientation near the isotropic-nematic crossover is strongly influenced by collective effects beyond those due to topological constraints on the motion, and in particular that there is significant coupling between rotational and translational diffusion, the only mechanism that, as discussed above, might lead to an increase in the rotational diffusion constant with increasing ν . With $\beta_r \sim 10^{-4}$, an enhancement of D_r in Eq. (7) by a factor ~ 6 would be required to give $D_r^* \geq D_{r0}$. The discrepancy between the experimental values for D_r^* from an analysis by Eqs. (5) could indicate that the enhancement itself depends on the degree of orientational order in the system. This would not be too surprising since both the potential U_{MF} and the translational diffusion D_1 are functions of S . In any case, a calculation of orientational relaxation based on the full dynamical equation (4) would be quite useful. Further, because of their unusually large size, one may have to consider more explicitly the coupling of the tubule orientational dynamics to flows in the solvent.

We next present results for $S(t)$ as a function of temperature for $T \rightarrow T_m$, the lipid chain-melting point. In Ref. [7], we report a quite substantial range of pretransitional decrease in the maximum induced index anisotropy Δn_{\max} for $\rho \leq 2.0$ mg/cm³; as Fig. 2 of the present work demonstrates, we observe a broad temperature dependence in the reorientation dynamics as well. In both cases, T was always changed in high field. As discussed in Ref. [7], the substantial range of pretransitional change in Δn_{\max} suggests a continuous reduction of the tubule anisotropy; we do not, however, believe it to represent any true critical behavior at the tubule-isotropic phase transition for $\rho \leq 2.0$ mg/cm³. The decay time after removal of the field decreases strongly with increasing T , and the decay is increasingly single exponential. From this dependence, we find (see the solid lines in Fig. 2) $D_r = 3.5 \times 10^{-4}$, 1.4×10^{-3} , and 4.0×10^{-3} sec⁻¹ for $T = 25.95$, 29.40 , and 31.77 °C, respectively. Also, at higher temperatures, where Δn_{\max} has significantly decreased [7], there is substantial reorientation while the

field is being swept away; indeed, for $|T - T_m| \approx 0.6^\circ\text{C}$, S drops to about 0.35 during this time.

To account for these effects, we consider possibilities for the transformation of the tubules when $T \rightarrow T_m$. The marked increase in D_r with T strongly points to a structural evolution of the tubules. In fact, in pure water systems, evidence from microscopy [5] suggests a transformation to spherical liposomes at T_m . For weakly aqueous dispersions, our results for Δn_{\max} as a function of T [7] indicate a substantial range of pretransitional behavior in high field, and an isotropic system above T_m (no induced Δn). Here we shall briefly discuss two scenarios for the pretransitional behavior. We assume, consistent with electron-microscopy observations [6,8], that the tubules in the weakly aqueous system are formed of helically wound bilayer ribbons that are fused at the edges. In the first scenario, we envision a uniform collapse of the pitch of the winding with increasing T , resulting in a more isotropic cylindrical structure with the same surface area $A_S = \pi bL$. Hence L decreases and b increases with the product bL remaining approximately constant. Then $1/bL^2 \approx \pi/A_S L$ increases and, since the particle concentration remains the same, ν is pushed toward the semidilute regime, where collective effects should be reduced. We then expect that the form of the decay after $H=0$ should approach a simple exponential, as is evidently the trend in Fig. 2. Moreover, the decay rate, $D_r \propto D_{r0} \propto L^{-3}$, will be strongly increasing for decreasing L , as observed. As a caveat, we point out that Eq. (7) for D_{r0} is only valid for $L \gg b$; thus the relation $D_{r0} \propto L^{-3}$ would be expected to break down sufficiently close to T_m (where the induced $\Delta n \rightarrow 0$ [7]).

Because of the increase in D_r as $T \rightarrow T_m$, any behavior for small t that is not a simple exponential will be suppressed to shorter times, perhaps eventually within the field-sweep interval. In fact, at the highest T in Fig. 2, most of the decay occurs within the sweep interval, and, although this may simply derive from the driving effect of the changing field combined with the large D_r estimated from the solid line after $H=0$, we can consider the possibility that a short-time relaxation arising from a structural evolution is involved for small Δn_{\max} . (The mechanism of Eq. (5a) applies only for very anisotropic hard rods—i.e., large Δn_{\max} .) If the tubules in a weakly aqueous environment transform by first dissociating into loose or “open” helical fragments that have substantial gaps between the bilayer edges [6,8], the structures near T_m might be rather flexible. This flexibility could, in turn, lead not only to an increase in D_r , but also to a “stretching” distortion of the helix whose relaxation time during removal of a large field would be very rapid (i.e., limited by the sweep time itself) compared to a rotational diffusion process dominating at longer times. Of course, to test this conjecture, detailed short-time data must be obtained, perhaps with the use of pulsed fields.

Finally, we remark on an unusual and potentially interesting observation. Figure 2 also shows the dynamical response when $H \rightarrow 0$ after cooling the system from $T > T_m$ to the original temperature $T = 18.61^\circ\text{C}$. The same temperature steps were used for heating and cool-

ing, and all temperature changes were made in high field. Moreover, after cooling we recovered a value of Δn_{\max} very close to that measured prior to heating [7]. Based upon the static data, one might therefore assume that the original tubules had reformed. However, the dynamical behavior, as Fig. 2 reveals, indicates otherwise. Over a range of t during which Δn for the original tubules decays by almost e^{-2} , there is *no* change in Δn in the reformed system. One possibility for this behavior is a large hysteresis in the reformation process; the structure after cooling, which itself is quite anisotropic, may be metastable, producing the original tubules only after a sufficiently long time (during which Δn would eventually decay). The exposure to the high field during cooling may play an important role in this metastability, a scenario we are currently investigating. Alternatively, the tubules in the reformed system may for some reason be longer. Since the actual concentration $\nu \sim 1/(\delta bL)$ but the threshold $\nu^* \sim 1/(bL^2)$, a sufficient increase in L may result in $\nu > \nu^*$, placing the system into the nematic regime so that Δn would be stable. Because $\Delta n_{\max} \sim \nu L$ [17] for $L \gg b$ (and $\nu \sim 1/L$), the level of anisotropy might not change much. Electron microscopy and DLS experiments, which would probe the system immediately after cooling from $T > T_m$ in high field, are planned to help resolve this issue.

We now discuss DLS results obtained in zero field. A solution with initial lipid density $\rho = 1.0 \text{ mg/cm}^3$ was used in order to limit multiple scattering yet maintain a tubule concentration in the same regime for hard-rod dynamics, $\nu \sim 1/(bL^2)$, as that studied in our MB experiment. We therefore expect the relative contributions of the diffusion constants D_r^* , D_\perp^* and D_\parallel^* to be similar in the two experiments. Homodyne correlation functions were collected at a 45° scattering angle and normal incidence, giving $q^2 = 5.34 \times 10^9 \text{ cm}^{-2}$. The sample thickness was $500 \mu\text{m}$, chosen to minimize multiple scattering while preserving a three-dimensional system. The possibility of multiple scattering was checked by measuring the forward extinction through the sample. At 22°C we measured 95% transmission; this corresponds to an optical path $\tau = 0.05$, which is below the threshold $\tau \sim 0.1-0.3$ for significant multiple scattering [27]. Results for three temperatures below T_m and two above T_m are presented in Fig. 3. The solid lines are fits of the intensity-intensity autocorrelation function to a three-cumulant analysis, Eq. (8); the background was always fixed to the measured value.

As in the case of the relaxation of $S(t)$ (Fig. 2), we observe a quite clear temperature dependence for $T \rightarrow T_m$; we obtain $\Gamma_1/q^2 = 4.4 \times 10^{-10}$, 6.4×10^{-10} , and $8.2 \times 10^{-10} \text{ cm}^2/\text{sec}$, and $\mu_2/\Gamma_1^2 = 0.83$, 0.67 , and 0.34 , for $T = 22.08$, 27.95 , and 31.94°C , respectively. Using the experimental Γ_1/q^2 at 22.08°C and Eqs. (9), we may extract values of D_r^* in the two limits discussed previously, $D_\perp^* \ll (L^2/12)D_r^*$ and $D_\parallel^* \approx (L^2/12)D_r^*$. We get $D_r^* = 1.5 \times 10^{-4}$ and $7.3 \times 10^{-5} \text{ sec}^{-1}$. The former is comparable to the low-temperature values obtained from the MB data (Fig. 2) at large times, $D_r^* = (1.1-3.5) \times 10^{-4} \text{ sec}^{-1}$ for $T = 18.6-26.0^\circ\text{C}$, al-

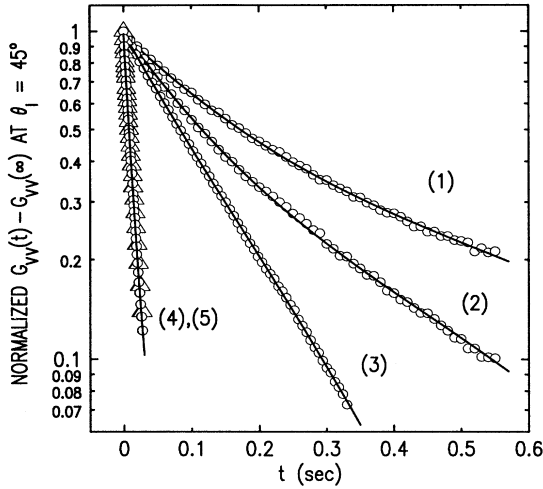


FIG. 3. Semilog plots of the normalized value of $G_{VV}(t) - G_{VV}(\infty)$ for $\theta_1 = 45^\circ$ as a function of temperature for $T \rightarrow T_m$ and $\rho = 1.0 \text{ mg/cm}^3$. The labels (1)–(3) indicate temperatures $T = 22.08, 27.95,$ and 31.94°C , respectively. The solid lines are fits to Eq. (8) of the text. Data above T_m at $T = 33.99$ and 35.06°C are indicated by the labels (4) (circles) and (5) (triangles).

though the tubule concentration in the two experiments differs by a factor of 2. We should also caution that the MB value was obtained for a system with $S > 0.2$, whereas the DLS measurement was made when $S \sim 0$. Nor is it clear on theoretical grounds [19] if the two values, which presumably account for collective diffusion effects, should be comparable when $qL \gg 1$ for DLS and $q \sim 0$ for MB. Perhaps a more revealing parameter is the normalized dispersion, μ_2/Γ_1^2 . Equations (9) also give $\mu_2/\Gamma_1^2 = 0.8$ and 0.2 for $D_\perp^* \ll (L^2/12)D_r^*$ and $D_\perp^* \approx (L^2/12)D_r^*$, respectively; the former agrees better with the experimental value 0.83 at $T = 22.08^\circ\text{C}$.

As previously noted, tubules formed in methanol-water solution are of very uniform size; we therefore do not expect polydispersity to account for a large μ_2 . Assuming $\Delta L/L \leq 0.1$ for the distribution in L at 22°C (see above), we may estimate the impact of polydispersity as follows. In the worst case [$\beta_r(\nu L^3)^2 \gg 1$ in Eq. (6)], $D_r \propto 1/(\nu^2 L^9) \propto 1/L^7$. Then, from Eqs. (9) for both limiting cases of D_\perp considered, the contribution to μ_2/Γ_1^2 at 22°C from polydispersity could be as much as $(\Delta\Gamma_1/\Gamma_1)^2 \approx (5\Delta L/L)^2 \sim 0.2$. This is still fairly small compared to the measured value of 0.8 [however, it is comparable to the predicted μ_2/Γ_1^2 for the limit $D_\perp^* \approx (L^2/12)D_r^*$ in Eqs. (9)].

These results support the validity of Eqs. (9) for $qL \gg 1$ and $T \ll T_m$ (for fully formed tubules), and seem more consistent with $D_\perp^* \ll (L^2/12)D_r^*$. For $T \rightarrow T_m$, we observe that the measured Γ_1 for $\rho = 1.0 \text{ mg/cm}^3$ increases more slowly than D_r^* obtained for $\rho = 2.0 \text{ mg/cm}^3$. This may indicate that the details of the tubule transformation at T_m differ in the two experiments due to the different positions of the two concentrations in the phase diagram for the system. Alternatively, if

$\Gamma_1/q^2 \propto L^2 D_r^*$, the structural transformation may be similar (as is indicated in the high-field results of Ref. [7]), and the different rates of change for Γ_1 and D_r^* may simply reflect different dependences on a decrease in the effective value of L . Moreover, the nonexponential character of G_{VV} is reduced for $T \rightarrow T_m$. A reduction in L accompanying the decrease in μ_2/Γ_1^2 at higher T is consistent with the results of Ref. [14] on a rigid-rod polymer system. There, a crossover from strong to weak nonexponential behavior was found as νL^3 dropped below ~ 300 . Using $\nu \sim 2 \times 10^9 \text{ cm}^{-3}$ and $L = 6 \times 10^{-3} \text{ cm}$ for the original tubules, we get $\nu L^3 \sim 430$, so that a modest decrease in L could lead to a marked change in the character of G_{VV} . Finally, a difference in the observed rate of increase of D_r^* and Γ_1 with T may arise in part due to increased two-dimensional confinement of the tubules; in the light-scattering experiment, the cell thickness was only ~ 10 times the initial tubule length.

At the higher temperatures $T = 33.99$ and 35.06°C , we observe a much faster decay, which has $\Gamma_1/q^2 = 9.1 \times 10^{-9} \text{ cm}^2/\text{sec}$ for both temperatures. Evidently, a sharp change in the dynamics occurs for $T \sim T_m \approx 33.2^\circ\text{C}$. If we assume that above T_m the structure is qualitatively different—specifically, that the system consists of nearly spherical particles or aggregates (e.g., vesicles), which is consistent with $\Delta n_{\text{max}} \sim 0$ [7]—we may estimate their mean radius from the well-known prediction for single spheres, $\Gamma_1/q^2 = k_B T / (6\pi\eta_S R)$ [29]. This also assumes that the particles are rigid (i.e., no intraparticle motion, which for $R \sim \lambda$ could scatter light), and that there are no significant interactions. We find $R \approx 0.24 \mu\text{m}$, a very large value, which, based on the results of previous work [2,7] for $\rho = 1.0 \text{ mg/cm}^3$, should lead to a higher sample turbidity than we observe. We find for the normalized dispersion of G_{VV} , $\mu_2/\Gamma_1^2 \approx 0.5$, which is about 20% higher than typically found for large vesicles [30]. These results suggest that a model of rigid, noninteracting spheres at $T > T_m$ and for the initial lipid densities $\rho < 2.0 \text{ mg/cm}^3$ studied in Refs. [2] and [7] may be naive, and point to the need for a detailed study of the q dependence of both the amplitude and decay constant associated with the scattering, as a basis upon which to evaluate models of the structure at $T > T_m$. (For example, particles of size R with $qR \sim 1$ should have a non-trivial scattering form factor.)

To conclude, we have reported results for the dynamical behavior of highly concentrated solutions of phospholipid tubules on approach to the lipid chain-melting temperature. From MB experiments, we have obtained at $T \ll T_m$ a value of the hard-rod rotational diffusion constant that is larger than that predicted strictly from rod entanglement effects in a homogeneous zero-field system, suggesting that substantial coupling to translational diffusion is involved in the rotational dynamics for the very high concentration studied. DLS data for $T \ll T_m$ support a theoretical calculation of the intensity-intensity autocorrelation function for scattering from hard rods when $L \gg \lambda$, and are reasonably consistent with the low- T MB results when the orientational order parameter S is small. For $T < T_m$, the decay of $S(t)$ after removal of a

saturating field shows short-time behavior, which, as theoretically predicted for high fields, is not a simple exponential, and asymptotic behavior that is consistent with a pure exponential.

For $T \rightarrow T_m$, both the MB and DLS results show clear pretransitional effects, which indicate a structural change in the tubules, although much more complete dynamical data will be necessary to test specific models of the transformation, which have anyway yet to be fully developed. These experiments are underway, together with a DLS study of the behavior near T_m for different concentrations in the range where we report in Ref. [7] an interesting crossover in the shape of $\Delta n_{\max}(T)$. It would also be interesting to probe the dependence of the translational

diffusion on the magnitude of S induced by a high field. Finally, we might expect rather different pretransitional behavior in the dynamics of tubules formed in a purely aqueous solution.

We wish to acknowledge support from several sources. Two of us (B.R. and R.S.) were supported by the Office of Naval Research, while S.S. was supported by NSF Grant No. DMR-9111389, J.D.L. was supported by NSF Grant No. DMR-9014886, and G.N. was supported by the Naval Research Laboratory through Grant No. NRL N00014-91-J-2007. We also wish to thank Sangamitra Baral-Tosh for help in preparing tubule samples.

*Also at Department of Biochemistry, Georgetown University Medical Center, Washington, D.C. 20007.

- [1] P. Yager and P. E. Schoen, *Mol. Cryst. Liq. Cryst.* **106**, 371 (1984); P. Yager, P. E. Schoen, C. Davies, R. Price, and A. Singh, *Biophys. J.* **48**, 899 (1985); N. Nakashima, S. Asakuma, and T. Kunitake, *J. Am. Chem. Soc.* **107**, 509 (1985); J.-H. Fuhrhop, P. Schneider, E. Boekema, and W. Helfrich, *J. Am. Chem. Soc.* **110**, 2861 (1988).
- [2] B. R. Ratna, S. Baral-Tosh, B. Kahn, J. M. Schnur, and A. S. Rudolph, *Chem. Phys. Lipids* **63**, 47 (1992).
- [3] P.-G. de Gennes, *C. R. Acad. Sci. Paris* **304**, 259 (1987); W. Helfrich and J. Prost, *Phys. Rev. A* **38**, 3065 (1988); W. Helfrich, *J. Chem. Phys.* **85**, 1065 (1986).
- [4] M. Caffrey, J. Hogan, and A. S. Rudolph, *Biochemistry* **30**, 2134 (1991).
- [5] P. Yager, R. R. Price, J. M. Schnur, P. E. Schoen, A. Singh, and D. G. Rhodes, *Chem. Phys. Lipids* **46**, 171 (1988).
- [6] J. H. Georger, A. Singh, R. Price, J. M. Schnur, P. Yager, and P. E. Schoen, *J. Am. Chem. Soc.* **109**, 6169 (1987).
- [7] S. Sprunt, G. Nounesis, J. D. Litster, B. R. Ratna, and R. Shashidhar, *Phys. Rev. E* (to be published).
- [8] B. R. Ratna (unpublished).
- [9] M. Doi and S. F. Edwards, *The Theory of Polymer Dynamics* (Oxford University Press, London, 1986), Chaps. 8–10.
- [10] J. F. Maguire, J. P. McTague, and F. Rondelez, *Phys. Rev. Lett.* **45**, 1891 (1980); Y. Mori, N. Ookubo, R. Hayakawa, and Y. Wada, *J. Polym. Sci.* **20**, 2111 (1982).
- [11] K. M. Zero and R. Pecora, *Macromolecules* **15**, 87 (1982).
- [12] J. Wilcoxon and J. M. Schurr, *Biopolymers* **22**, 849 (1983).
- [13] K. Kubota, H. Urabe, Y. Tominaga, and S. Fujime, *Macromolecules* **17**, 2096 (1984).
- [14] P. Russo, F. Karasz, and K. Langley, *J. Chem. Phys.* **80**, 5312 (1984).
- [15] L. Onsager, *Ann. N.Y. Acad. Sci.* **51**, 627 (1949).
- [16] This is the value obtained from optical anisotropy measurements in zero field (see Ref. [7]).
- [17] This estimate is based on a combination of available data on the lipid head area in the tubule bilayer (Ref. [4]) and on the mass density of the bilayer [see M.-H. Lu and C. Rosenblatt, *Mol. Cryst. Liq. Cryst.* **210**, 169 (1992)].
- [18] Min-Hua Lu, Jerome B. Lando, J. Aden Mann, Jr., Rolfe G. Petschek, and Charles B. Rosenblatt, *Langmuir* **7**, 1988 (1991); Min-Hua Lu, Rolfe G. Petschek, and Charles Rosenblatt, *J. Colloid Interface Sci.* **142**, 121 (1991).
- [19] M. Doi, T. Shamada, and K. Okano, *J. Chem. Phys.* **88**, 4070 (1988).
- [20] M. Doi, *J. Polym. Sci.* **19**, 229 (1981).
- [21] M. Doi and S. F. Edwards, *J. Chem. Soc. Faraday Trans. 2* **74**, 560 (1978).
- [22] S. Broersma, *J. Chem. Phys.* **32**, 1626 (1960); **32**, 1632 (1960); J. Newman, H. Swinney, and L. Day, *J. Mol. Biol.* **116**, 593 (1977).
- [23] I. Teraoka, Y. Mori, N. Ookubo, and R. Hayakawa, *Phys. Rev. Lett.* **55**, 2712 (1985); M. Doi, I. Yamamoto, and F. Kano, *J. Phys. Soc. Jpn.* **53**, 3000 (1984).
- [24] R. Matheson, *Macromolecules* **13**, 643 (1980).
- [25] H. Nakamura and K. Okano, *Phys. Rev. Lett.* **50**, 186 (1983).
- [26] T. Maeda and S. Fujime, *Macromolecules* **17**, 1157 (1984).
- [27] H. C. van de Hulst, *Light Scattering by Small Particles* (Dover, New York, 1981), Chaps. 9 and 15.
- [28] V. Degiorgio, R. Piazza, F. Mantegazza, and T. Bellini, *J. Phys.: Condens. Matter* **2**, SA69 (1990).
- [29] Bruce J. Berne and Robert Pecora, *Dynamic Light Scattering* (Wiley, New York, 1976), Chap. 5.
- [30] See, e.g., J. C. Selser, Y. Yeh, and R. J. Baskin, *Biophys. J.* **16**, 337 (1976).